JVSTA Journal of Vacuum Science & Technology A

CO adsorption on Pd(111) and Pd(100): Low and high pressure correlations

János Szanyi, W. Kevin Kuhn, and D. Wayne Goodman

Citation: Journal of Vacuum Science & Technology A **11**, 1969 (1993); doi: 10.1116/1.578532
View online: http://dx.doi.org/10.1116/1.578532
View Table of Contents: http://scitation.aip.org/content/avs/journal/jvsta/11/4?ver=pdfcov
Published by the AVS: Science & Technology of Materials, Interfaces, and Processing

CO adsorption on Pd(111) and Pd(100): Low and high pressure correlations

János Szanyi, W. Kevin Kuhn, and D. Wayne Goodman[a)]
Texas A&M University, Department of Chemistry, College Station, Texas 77843-3255

(Received 30 September 1992; accepted 23 November 1992)

The adsorption of CO on Pd(111) and Pd(100) have been studied using infrared reflection–absorption spectroscopy over a wide range of CO pressures and temperatures. A strong dependence of CO adsorption on the initial conditions was found for Pd(111) while CO adsorption on Pd(100) was essentially independent of the conditions of adsorption. Initial isosteric heats of adsorption of 30 and 38 kcal/mol were determined for Pd(111) and Pd(100), respectively. For Pd(111) and equilibrium phase diagram was constructed on the basis of the infrared (IR) data. The excellent correspondence among IR data for the single crystal Pd surfaces and a supported Pd catalyst suggests that the Pd particles in the supported catalyst consist primarily of low index [(111) and (100)] crystal faces.

I. INTRODUCTION

In heterogenous catalytic processes the adsorption of one or more components of the reactant gas mixture is generally one of the most important steps of the catalytic cycle. Vibrational spectroscopies (infrared and electron energy-loss spectroscopies) have been utilized successfully to investigate adsorption of gas molecules on metal surfaces.[1–3] These studies, generally carried out under ultrahigh vacuum (UHV) conditions, have provided valuable information about the interaction of the adsorbate with the substrate as well as the geometry of the adsorbate–substrate complex. However, questions have been raised frequently regarding extrapolation of the information acquired in these studies to "real world" catalytic systems, i.e., high temperatures, high pressures, and high surface area supported catalysts. Of concern is the so-called "pressure gap" that exists between the UHV and the more realistic catalytic studies. In recent years significant steps toward closing this pressure gap have been made by utilizing combined elevated pressure reactor/UHV surface analysis systems.[4] *In situ* adsorption studies at elevated pressures utilizing infrared reflection–absorption spectroscopy (IRAS) have also been carried out recently.[5–7] In certain cases[8] these results have shown that data acquired under UHV conditions can be extrapolated to high pressure and high temperature conditions.

The adsorption of CO on Pd(111) and Pd(100) has been studied extensively under UHV conditions using a wide variety of analytical techniques. Carbon monoxide adsorbs molecularly on Pd surfaces, bound through the carbon end of the molecule.[9] The collective structure of the adsorbed CO is dependent upon the particular Pd crystal face. For example, on the Pd(111) surface, at CO coverages up to 1/3 monolayer (ML), CO adsorbs onto threefold hollow sites, with a structure corresponding to a $(\sqrt{3}\times\sqrt{3})R30°$ low-energy electron diffraction (LEED) pattern.[2,5] The carbon–oxygen stretching frequency of the threefold hollow adsorbed CO is $\sim 1850\ cm^{-1}$.[2] With increasing CO coverage, compressed CO structures are observed in LEED studies[9] and additional adsorption sites have been identified by infrared (IR).[2] At 0.5 ML, a $c(2\times2)$ LEED pattern and a vibrational frequency at 1918 cm^{-1} are observed, corresponding to CO adsorbed onto bridging sites. At high coverages, a-top and bridge-bound CO coexist producing a (2×2) LEED pattern; in IR two corresponding stretching frequencies are found at 1951 and 2097 cm^{-1}, respectively. However, in a temperature programmed desorption (TPD) study Guo and Yates[10] have shown that the desorption kinetics of CO from Pd(111) depend on the initial adsorption temperature and thus on the initial coverage.

CO adsorption on Pd(100), which has been studied extensively using an array of surface analysis techniques,[1,5,11–17] yields only the bridging site. LEED analysis[11,12,14,15] has shown that at a CO coverage of 0.5 ML, a $c(2\sqrt{2}\times\sqrt{2})R45°$ structure was evident. Above 0.5 ML a uniaxial compression takes place which results in the formation of a series of incommensurate overlayers.[12] As a consequence of this compression of the CO overlayer, a sharp decrease in the heat of CO adsorption at 0.5 ML was observed.[12,15]

IRAS studies[1,17] under low pressure conditions have also shown the bridging configuration of the adsorbed CO on Pd(100). The C–O stretching frequency shifts from ~ 1895 to $\sim 1950\ cm^{-1}$ as the CO coverage increases to 0.5 ML. At the commensurate–incommensurate transition an 11 cm^{-1} frequency shift was observed.[1] At CO coverages above 0.5 ML, the CO frequency continuously shifts toward higher values and reaches its maximum of 1995 cm^{-1} at 0.8 ML.

To obtain further information about the adsorption of CO on Pd(111) and Pd(100) surfaces, we have carried out an adsorption study over a wide pressure range of 10^{-7} to 10 Torr using a combined elevated pressure IR cell–UHV surface analysis system. The results obtained for Pd(100) together with previously reported data for Pd(111)[18] allow a direct correlation to be made among data acquired at low pressure/low temperature and high pressure/high temperature conditions.

a)Author to whom correspondence should be addressed.

 0734-2101/93/11(4)/1969/6/$1.00

II. EXPERIMENTAL

The experiments were carried out in an UHV surface analysis chamber (base pressure less than 5×10^{-10} Torr) connected to an IR cell which can be operated at elevated pressures. The UHV chamber used in this study and the spectrometer arrangement have been described in detail elsewhere.[19,20] Briefly, the UHV chamber is equipped with an array of surface analytical techniques [Auger electron spectroscopy (AES), low-energy electron diffraction (LEED), and temperature programmed desorption (TPD)] and electron beam heating and gas and metal dosing capabilities. The IR cell has CaF_2 windows and is connected to the UHV chamber through a double differentially pumped sliding seal. The configuration of the elevated pressure cell is similar to that discussed by Campbell *et al.*[20] This arrangement allows IR experiments in the pressure range of 10^{-8}–10^{3} Torr and also provides convenient access to the sample without opening the UHV chamber. The elevated pressure IR cell is connected to a gas handling system allowing elevated pressure catalytic reactions as well. The pressure in the IR cell was determined using an ionization gauge in the 10^{-8}–10^{-3} Torr region; a 10 Torr Baratron gauge was used to monitor pressures between 10^{-2} and 10 Torr.

The sample was resistively heated using a Ta heating wire spot welded to the back face of the crystal. The sample temperature was monitored via a W-5%Re/W-26%Re thermocouple. The manipulator used in this study was essentially the same as that described in Ref. 20 with the only difference being the sample holder rod. In these studies a double wall tube was used in which the void between the two tubes was continuously evacuated. This was necessary in order to maintain the outer tube at ambient temperature during the IR experiments at low temperatures.

The crystal surface was cleaned by the procedure described in Ref. 21. AES and LEED was used to verify the cleanliness and the long range order of the sample surface, respectively.

The IR spectra (8 cm^{-1} resolution) were acquired using 512 scans in the single reflection mode at an incident angle of 85° with respect to the surface normal. Background spectra were acquired at sample temperatures sufficiently high to eliminate any contribution from adsorbed CO. At a given temperature IRAS features of adsorbed CO were found by subtracting the corresponding background spectrum from the spectrum obtained at the temperature of interest.[8]

III. RESULTS AND DISCUSSION

A series of IR spectra of adsorbed CO obtained at a CO pressure of 10 Torr are shown in Fig. 1. At this CO pressure the background spectrum was collected at a sample temperature of 1000 K. Preliminary experiments indicated that this temperature was sufficiently high to ensure a CO-free Pd(111) surface, thus the background spectrum contained contributions only from the gas phase CO. The spectra shown were recorded in a sequence of decreasing temperature. The spectral features, based on earlier

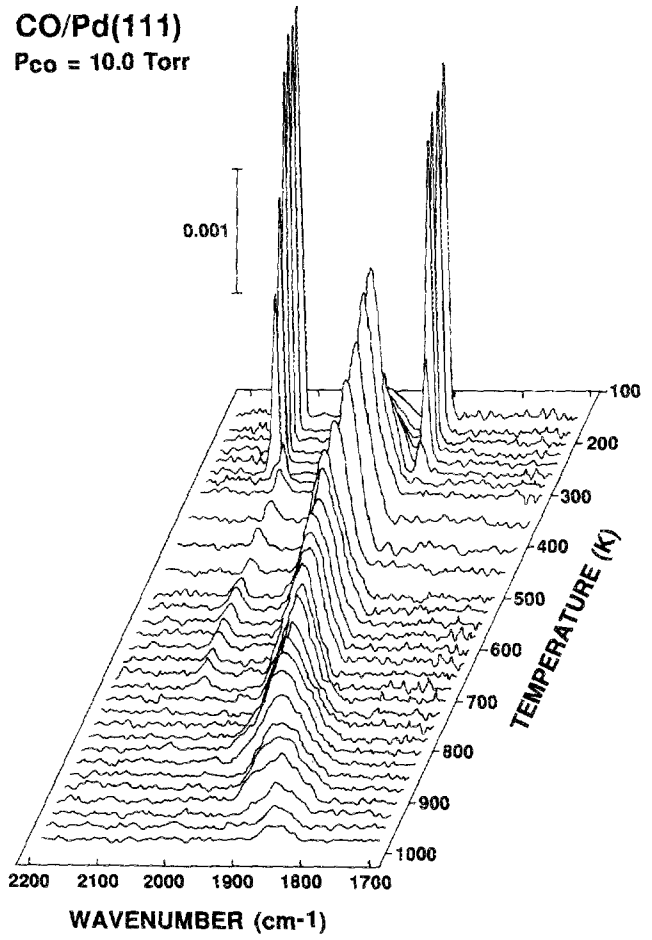

FIG. 1. The effect of temperature on the IR spectra of CO on Pd(111) at P_{CO} = 10 Torr. Reproduced with permission from Ref. 18.

studies[2] supplemented by our LEED observations, could be assigned to various structures of adsorbed CO. In agreement with previous results[2,22] three stages of CO adsorption can be identified in this series of spectra. At high temperatures (i.e., low CO coverages) the only sites occupied are the threefold hollows. With decreasing temperatures (i.e., increasing CO coverage) the bridging sites become increasingly more populated. At temperatures near 200 K, a sudden change in the spectrum is apparent, corresponding to a transition from adsorption onto the bridging sites to adsorption onto a mixture of atop and threefold hollow sites. The bridging→a-top/threefold hollow transition takes place in a very narrow temperature range while the transition from the threefold hollow to bridging sites is much less well-defined. The very narrow linewidths of the features assigned to the a-top and threefold hollow sites are also noteworthy. These very sharp peaks provide evidence for the presence of a well-ordered CO adsorbate layer on the Pd(111) substrate. LEED investigations, which showed a very sharp (2×2) pattern, indicated that this indeed was the case.

At a CO pressure of 10 Torr, temperatures of ~850–900 K for the threefold hollow→bridging transition and ~250 K for the bridging→a-top/threefold hollow transition are observed. The threefold hollow→bridging transi-

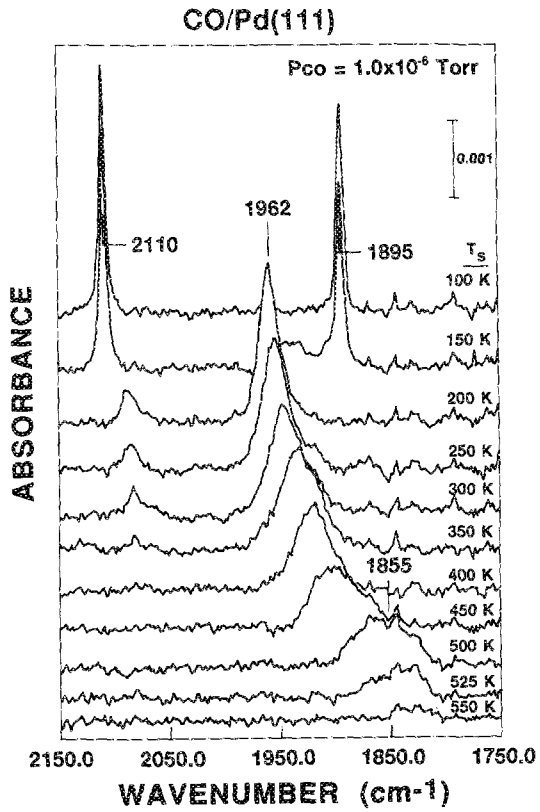

FIG. 2. IR spectra of CO on Pd(111) at $P_{CO} = 1\times10^{-6}$ Torr as a function of temperature. Reproduced with permission from Ref. 18.

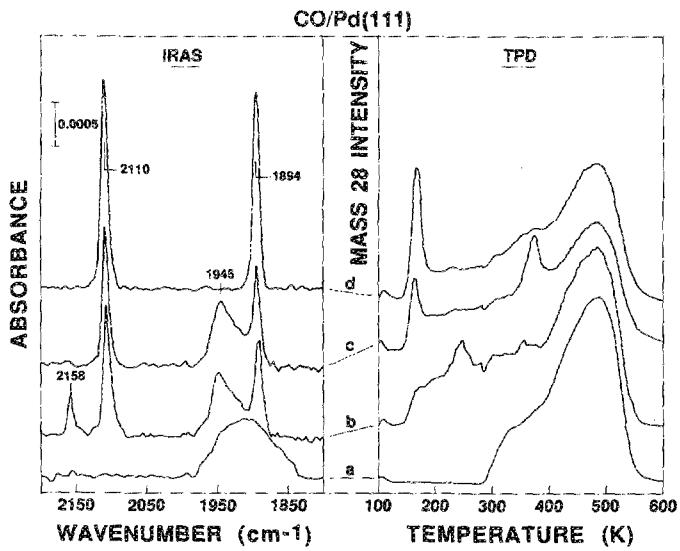

FIG. 3. IRAS and the corresponding TPD spectra of CO on Pd(111) as a function of annealing temperature at $P_{CO} = 1\times10^{-6}$ Torr. Sample temperature during the IR experiments was 90 K. Annealing temperatures were (a) 90 K, (b) 200 K, (c) 400 K, and (d) 600 K. Reproduced with permission from Ref. 18.

tion temperature is based on additional studies[1,2] at UHV conditions and elevated CO pressures. For example, in Fig. 2, in which the IR spectra were acquired at a CO pressure of 10^{-6} Torr, the transition from threefold hollow to bridging sites can clearly be seen as the CO stretching frequency changes from $\sim$1855 to $\sim$1900 cm^{-1}. As the population of the bridge-bound CO increases, the CO stretching frequency shifts toward higher values and the peak becomes sharper. The frequency shift can be attributed to the lateral interaction among adsorbed CO molecules, and the decrease in the peak width to a more highly ordered structure of the CO layer. The highest frequency observed for the bridge-bound CO was 1962 cm^{-1}. The frequencies of the a-top and threefold hollow CO molecules are 2110 and 1895 cm^{-1}, respectively. The frequency at which the threefold hollow CO can first be observed (i.e., the low coverage limit) is $\sim$1825 cm^{-1}. The corresponding frequency for the bridge-bound CO is $\sim$1950 cm^{-1}. Besides these well-defined, intense features, a small feature at 2096 cm^{-1} is evident in every spectrum. At a CO pressure of 10 Torr this feature appears first at $\sim$720 K and is present until the bridging$\rightarrow$a-top/threefold hollow transition at $\sim$250 K. This weak feature is likely due to a small amount of CO adsorbed onto a-top sites of Pd atoms and can be explained either by disorder in the CO overlayer or by the mismatch between the compressed CO (4×2) overlayer and the Pd(111) substrate that forces a small amount of CO into a-top positions.

In addition to the series of IR spectra acquired at a CO pressure of 10 Torr, IR spectra were collected at every decade of CO pressure from 1×10^{-6} to 10 Torr. Each series of spectra shows the progression of IR features seen at $P_{CO} = 10$ Torr. Although the progression of features are identical for each series, the transition temperature between the CO adsorption sites changes with the CO pressure. For $P_{CO} = 1\times10^{-6}$ Torr Fig. 2 displays a series of IR spectra collected with decreasing adsorption temperature. The temperature at which any CO feature is observed is 550 K at $P_{CO} = 1\times10^{-6}$ Torr, approximately 400 K lower compared with a CO pressure of 10 Torr. As noted above, the threefold hollow$\rightarrow$bridging transition is well-defined in this series of spectra and takes place between 450 and 500 K. Also the bridging$\rightarrow$a-top/threefold hollow transition shifts to lower temperature, i.e., to $\sim$150 K at 1×10^{-6} Torr from 250 K at 10 Torr. Using the data obtained at different CO pressures, isosteric heats of adsorption can be derived for various CO coverages. Accordingly, an initial heat of adsorption of 30 kcal/mol was determined, in excellent agreement with previously published data.[10,22]

The structure of the adsorbed CO layer on the Pd(111) surface is strongly dependent upon the initial adsorption conditions. In a recent TPD study Guo and Yates[10] observed markedly different behavior in the kinetics of CO desorption for CO overlayers adsorbed at 87 and 200 K. The effect of the adsorption conditions on the IRAS and TPD spectra of CO on Pd(111) is shown in Fig. 3. Figure 3(a) shows the IR and the corresponding TPD spectrum acquired after CO adsorption at 90 K and 10^{-6} Torr. For acquisition of the IRAS spectra, the CO pressure was maintained at 1×10^{-6} Torr. Upon completion of the IR spectrum the IR cell was evacuated to $<10^{-8}$ Torr and the sample transferred into the UHV surface analysis chamber. IR spectra acquired at 1×10^{-6} Torr CO pres-

sure and 90 K were identical to the one obtained after evacuation of the IR cell, suggesting no apparent change in the adsorbed CO layer following the removal of gas phase CO. Spectra *b*, *c*, and *d* were acquired at a CO pressure of 10^{-6} Torr, following an anneal of the sample to 200, 400, and 600 K, respectively. Following the anneal the sample was cooled to 90 K in 1×10^{-6} Torr of CO and the IR spectrum recorded. The corresponding TPD spectra were acquired following the preparation used for the data of Fig. 3. TPD spectra *a* and *b* agree well with previous results[11] showing a primary desorption feature at 500 K with a broad desorption tail extending down to 200–300 K. Both the IR and TPD spectra acquired after annealing and cooling to 90 K are distinctly different compared to the unannealed sample. Following saturation of the Pd(111) surface with CO at 90 K, only bridge-bound CO was observed. The very broad IR feature further suggests a CO overlayer that is not highly ordered. Annealing the sample in CO to progressively higher temperatures resulted in the disappearance of the bridge-bound CO species and the evolution of the a-top/threefold hollow CO. This is not a simple structural transformation of bridge-bound to a-top/threefold hollow CO. During the annealing process, an additional quantity of CO adsorbs on the surface, i.e., the CO coverage increases. No change in the 90 K IR spectrum was seen for a sample prepared at 90 K in 1×10^{-6} Torr CO, followed by an anneal in vacuum to 200 K. In both spectra only bridge-bound CO features were present which suggests that no bridge→threefold hollow reordering takes place during an anneal in vacuum. In the absence of gas-phase CO the saturation CO coverage at 90 K is sufficiently low to prevent the formation of the a-top/threefold hollow configuration. In addition to the IR data, TPD results also suggest an increase in CO coverage following an anneal in a CO background in that the total integrated CO mass spectral intensity for the annealed surface was about 10%–20% higher than that for the unannealed surface. A comparison of spectra *c* and *d* indicates that the desorption peak at 370 K in TPD spectrum *c* can be attributed to the bridging CO on the predominantly a-top/threefold hollow CO-covered surface. In the corresponding IR spectrum the presence of bridge-bound CO can clearly be seen as a feature at 1945 cm^{-1}. The absence of bridge-bound CO on the 600 K annealed sample is indicated by the absence of an IR feature at 1945 cm^{-1} and the absence of a desorption feature at 370 K.

In Fig. 4 an equilibrium phase diagram for CO on Pd(111) is reproduced, based on the adsorption data collected at temperatures between 90 and 1000 K and at CO pressures between 10^{-7} and 10 Torr. It should be emphasized that this phase diagram is valid only for the fully equilibrated adsorbate overlayers. This is especially the case for the bridging→a-top/threefold hollow phase transition. Nonequilibrium CO adsorption can occur at low adsorption temperatures as is apparent in Fig. 3. The region where nonequilibrated CO adsorption can take place is cross hatched in Fig. 4. In this region appropriate initial adsorption conditions have to be employed in order to obtain a fully equilibrated adsorbate overlayer. This equilibrium phase diagram, however, does illustrate that low pressure/low temperature adsorption information can be extrapolated into the high pressure/high temperature regime provided that certain initial adsorption conditions are used.

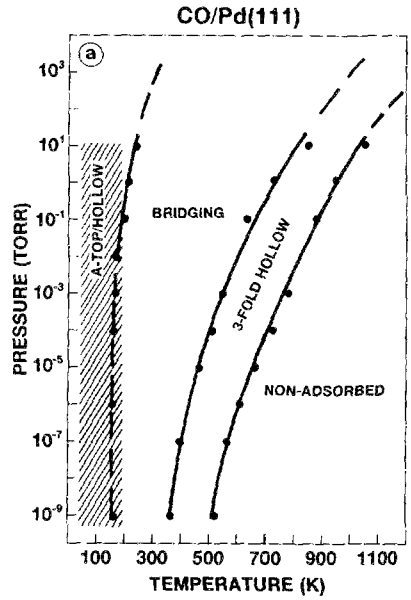

FIG. 4. Equilibrium pressure-temperature phase diagram for CO adsorption on Pd(111). Reproduced with permission from Ref. 18.

The adsorption of CO was also studied on Pd(100) in the pressure range of 10^{-7}–10 Torr. IR spectra were acquired under isobaric conditions at every decade of CO pressure following the same procedure described for Pd(111). Figure 5 displays two series of IR spectra collected at CO pressures of 10^{-6} and 1 Torr. In agreement with previous studies[12,17] only bridge-bound CO was seen throughout the temperature and pressure range investigated. A CO stretching frequency of 1895 cm^{-1} was observed at the lowest CO coverage with the frequency shifting toward higher values as the coverage was increased from 0 to 0.5 ML. The vibrational frequency that corresponds to a CO coverage of 0.5 ML is approximately 1950 cm^{-1}. Upon increasing the CO coverage above 0.5 ML, a sharp increase (~10 cm^{-1}) in frequency is apparent. This increase corresponds to a commensurate–incommensurate transition of the adsorbed CO layer resulting in a compressed overlayer structure. This transition has been discussed in detail by Ortega *et al.*[17] and recently by Brendt and Bradshaw.[23] The CO stretching frequency shifts continuously toward higher values as the coverage is increased from 0.5 ML to a maximum of $\sim$0.8 ML. Its value at the maximum CO coverage is 1995–1998 cm^{-1}. The IR peaks are sharper above the CO coverage of 0.5 ML suggesting a more highly ordered phase at these higher coverages. In contrast to the findings of Ortega *et al.*,[17] the integrated IR peak intensities did not plateau at CO coverages above 0.5 ML. At the point of transition to the compressed overlayer structure, a decrease in the integrated IR peak intensities is observed. Subsequent to the transition to this compressed structure, the integrated intensity increased monotonically

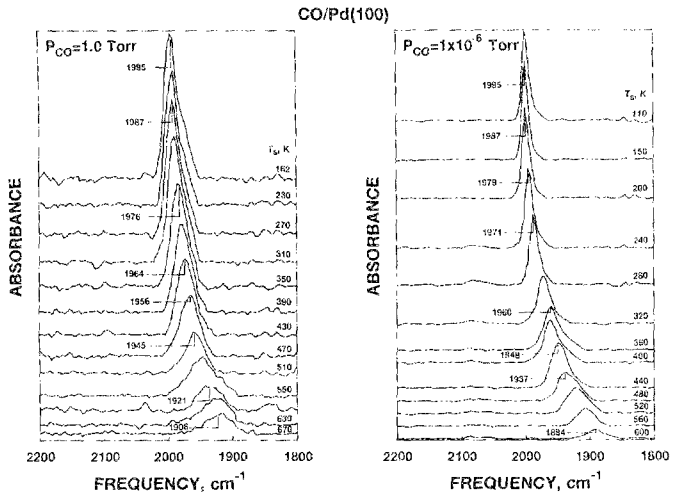

FIG. 5. IRAS spectra of CO on Pd(100) as a function of sample temperature at CO pressures of (a) 1 Torr and (b) 1×10^{-6} Torr.

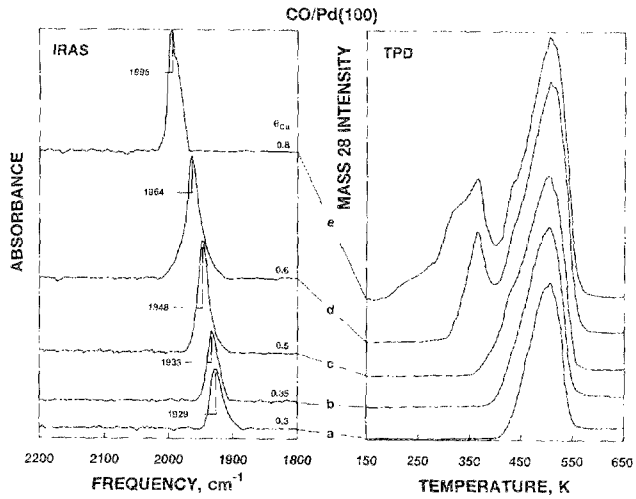

FIG. 6. Correlation between IRAS and TPD spectra of CO on Pd(100) as a function of CO coverage.

until the saturation CO coverage of 0.8 ML was reached. This uncertainty within the transition region regarding the CO IR cross section makes the acquisition of an isosteric heat of adsorption impossible to acquire accurately at high CO coverages. At low CO coverages, 38 kcal/mol was determined for the isosteric heat of adsorption, a value in good agreement with earlier literature values.[14,15,24]

Figure 6 shows a series of IR spectra and the corresponding TPD spectra for CO coverages between 0.3 and 0.8 ML. Below 0.5 ML only one desorption state was observed with a desorption peak maximum at ~500 K. Compression of the CO overlayer caused by the adsorption of additional CO results in a second feature at 370 K, indicating the collective instability of the compressed CO overlayer above 0.5 ML. This reduced stability is a result of movement of the CO molecules from the ideal bridging sites to the energetically less stable bonding positions as proposed in Refs. 17 and 23.

It has been proposed frequently that metal particles formed during the preparation of supported metal catalysts have structures dominated by the low index planes. Clearly, the formation of these low index planes [(100) and (111) in the case of Pd primarily] is energetically favored. If this is indeed the case, experiments using CO as a probe molecule could provide valuable information about the surface structures of small Pd particles in supported catalysts. In Fig. 7 IR spectra are shown for various Pd samples following a saturation exposure of CO. Spectra *a* and *b* were obtained from Pd(111) and Pd(100) single crystal surfaces, respectively, while spectrum *c* was acquired for a silica supported Pd catalyst (taken from Ref. 25). The features in the CO stretching region at 2103, 1995, and 1883 cm^{-1} observed for the supported Pd catalyst can be assigned to CO adsorbed in a-top, bridging, and threefold hollow positions, respectively. These frequencies agree very closely with CO frequencies found for CO adsorbed onto Pd(100) and Pd(111) surfaces. These characteristic CO IR results suggest that the metal particles present on the surface of the silica support have a significant population of (100) and (111) crystal faces. These results, however, are strictly qualitative. Any quantitative conclusions about the distribution of crystallites for model Pd supported particles must await a more complete characterization of these material with scanning tunneling microscopy (STM). Such studies are in progress.

IV. SUMMARY

Adsorption studies of CO on Pd(111) have shown that initial adsorption conditions greatly alter the IR and TPD spectra of CO. On the other hand, the CO adsorption characteristics for Pd(100) were independent of the initial adsorption conditions. These results suggest that great care must be taken in extrapolating data obtained under low

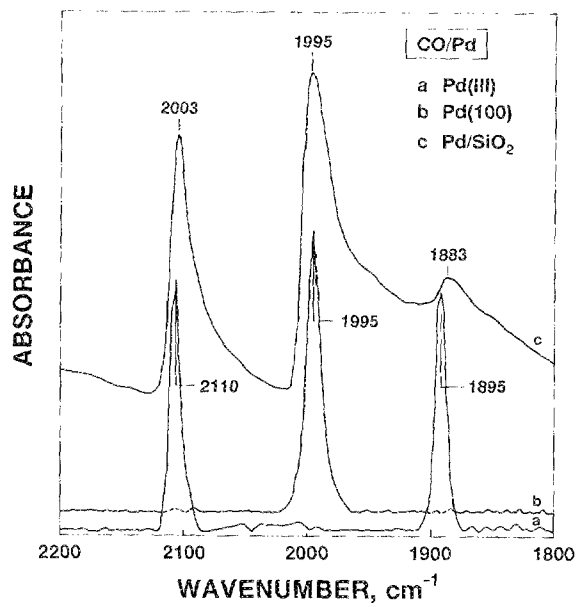

FIG. 7. Comparison of equilibrium IR spectra of CO on Pd(111) (a), Pd(100) (b) and a silica supported Pd catalyst (c). (Spectrum *c* was obtained from Fig. 4. of Ref. 25.)

temperature/low pressure conditions to the high pressure/high temperature regime. For Pd(111) an equilibrium phase diagram shows the continuity of CO adsorption phases with increasing pressure and temperature. Initial isosteric heats of adsorption of 30 and 38 kcal/mol were determined for Pd(111) and Pd(100), respectively. A remarkably good agreement was found among IR spectra of CO for Pd(111) and Pd(100) single crystals and a silica supported Pd catalyst. The comparison of IR spectra for these systems suggests that the Pd crystallites on the supported catalyst surface consists primarily of (111) and (100) crystal faces.

ACKNOWLEDGMENTS

We acknowledge with pleasure the support of this work by the Department of Energy, Office of Basic Energy Sciences, Division of Chemical Sciences, and the Robert A. Welch Foundation.

[1]A. M. Bradshaw and F. M. Hoffmann, Surf. Sci. **72**, 513 (1978).
[2]F. M. Hoffmann, Surf. Sci. Rep. **3**, 107 (1983).
[3]E. G. H. Froitzheim, H. Ibach, and S. Lehwald, Phys. Rev. Lett. **36**, 1549 (1976).
[4]J. A. Rodriguez and D. W. Goodman, Surf. Sci. Rep. **14**, 1 (1991), and references therein.
[5]*In Situ Methods in Catalysis, Catal. Today*, edited by R. Burch (Elsevier, Amsterdam, 1991), Vol. 9.
[6]F. M. Hoffmann and J. L. Robinson, J. Vac. Sci. Technol. A **5**, 724 (1987).
[7]C. H. F. Peden, D. W. Goodman, M. D. Weisel, and F. M. Hoffmann, Surf. Sci. **253**, 44 (1991).
[8]C. M. Truong, J. A. Rodriguez, and D. W. Goodman, Surf. Sci. Lett. **271**, L385 (1992).
[9]H. Conrad, G. Ertl, J. Koch, and E. E. Latta, Surf. Sci. **43**, 462 (1974).
[10]X. Guo and J. T. Yates, J. Chem. Phys. **90**, 6761 (1989).
[11]R. L. Park and H. H. Madden, Surf. Sci. **11**, 188 (1968).
[12]J. C. Tracy and P. W. Palmberg, J. Chem. Phys. **51**, 4852 (1969).
[13]J. P. Barta, K. Hermann, A. M. Bradshaw, and K. Horn, Phys. Rev. B **20**, 801 (1978).
[14]R. J. Behm, K. Christmann, G. Ertl, M. A. Van Hove, P. A. Thiel, and W. H. Weinberg, Surf. Sci. **88**, L59 (1979).
[15]R. J. Behm, K. Christmann, G. Ertl, and M. A. Van Hove, J. Chem. Phys. **73**, 2984 (1980).
[16]N. R. Avery, J. Chem. Phys. **74**, 4202 (1981).
[17]A. Ortega, F. M. Hoffmann, and A. M. Bradshaw, Surf. Sci. **119**, 79 (1982).
[18]W. K. Kuhn, J. Szanyi, and D. W. Goodman, Surf. Sci. **274**, L611 (1992).
[19]L.-W. Leung, J.-W.He, and D. W. Goodman, J. Chem. Phys. **93**, 8378 (1990).
[20]R. A. Campbell and D. W. Goodman, Rev. Sci. Instrum. **63**, 172 (1992).
[21]M. Grunze, H. Ruppenderand, and O. Elshazly, J. Vac. Sci. Technol. A **6**, 1266 (1988).
[22]H. Conrad, G. Ertl, and J. Küppers, Surf. Sci. **76**, 323 (1978).
[23]W. Brendt and A. M. Bradshaw, Surf. Sci. Lett. **279**, L165 (1992).
[24]J. C. Tracy and P. W. Palmberg, Surf. Sci. **14**, 274 (1969).
[25]P. Gelin, A. R. Siedle, and J. T. Yates, J. Phys. Chem. **88**, 2978 (1984).